Jpn J Radiol
DOI 10.1007/s11604-014-0322-0

ORIGINAL ARTICLE

# High-signal-intensity abnormalities evaluated by 3D fluid-attenuated inversion recovery imaging within the drainage territory of developmental venous anomalies identified by susceptibility-weighted imaging at 3 T

**Maki Umino · Masayuki Maeda · Nobuyoshi Matsushima · Keita Matsuura · Tomomi Yamada · Hajime Sakuma**

Received: 2 March 2014 / Accepted: 16 April 2014
© Japan Radiological Society 2014

**Abstract**
*Purpose* To evaluate brain parenchymal high-signal-intensity abnormalities within the drainage territory of developmental venous anomalies (DVAs) identified by susceptibility-weighted imaging (SWI) at 3 T.
*Methods* One hundred and thirty patients with 137 DVAs identified by SWI were retrospectively studied. 3D fluid-attenuated inversion recovery (FLAIR) images were reviewed for parenchymal high-signal-intensity abnormalities and SWI images were reviewed for hypointense foci (microhemorrhages or cavernous malformations) adjacent to DVAs. Patient age, the degree of underlying white matter disease, DVA location (supratentorial or infratentorial), and the presence or absence of hypointense foci were compared across DVAs with and without high-signal-intensity abnormalities. The correlation between patient age and the size of any high-signal-intensity abnormality was analyzed using linear regression.
*Results* Forty-two of 137 DVAs (30.7 %) had high-signal-intensity abnormalities. An adjusted prevalence of 18/71 (25.4 %) was obtained after excluding patients with considerable underlying white matter disease. Only DVA location (supratentorial) was associated with the presence of high-signal-intensity abnormalities ($p < 0.05$). There was a significant correlation between patient age and the size of high-signal-intensity abnormalities ($p < 0.01$).
*Conclusions* 3D FLAIR imaging permits detection of small high-signal-intensity abnormalities within the drainage territory of DVAs. The size of high-signal-intensity abnormalities increased with patient age.

**Keywords** Magnetic resonance imaging · Susceptibility-weighted imaging · Developmental venous anomalies · Fluid-attenuated inversion recovery · Parenchymal high-signal-intensity abnormalities

M. Umino (✉) · M. Maeda · N. Matsushima · H. Sakuma
Department of Radiology, Mie University School of Medicine, 2-174 Edobashi, Tsu, Mie 514-5807, Japan
e-mail: m-tochio@clin.medic.mie-u.ac.jp

K. Matsuura
Department of Neurology, Suzuka Kaisei Hospital, 112-1 Koucho, Suzuka, Mie 513-0836, Japan

T. Yamada
Department of Clinical Epidemiology and Biostatistics, Osaka University School of Medicine, 2-2 Yamadaoka, Suita, Osaka 565-0871, Japan

## Introduction

Developmental venous anomalies (DVAs), also referred to as venous angiomas or cerebral medullary venous malformations, are the most common vascular malformation of the brain [1–3]. Lasjaunias et al. interpreted them as extreme anatomical variants of the medullary venous system [4], whereas Okudera et al. concluded that they arose from aplasia, hypoplasia, or occlusion of the various segments of the superficial or deep drainage medullary veins or distal pial vein immediately before opening into the dural sinus [5]. They are typically diagnosed incidentally during imaging investigations for unrelated symptoms.

Although the parenchyma drained from a DVA is usually normal brain tissue, there have been reports of parenchymal abnormalities within the drainage territory of a DVA. The most frequently encountered abnormalities are cavernous malformations (CMs) or hemorrhage, which have been reported for 13.3–62.3 % of DVAs [2, 6, 7]. Abnormally high signal intensity on 1.5-T MR images has been reported for 7.8–28 % of DVAs [6, 8] and, in a recent

Published online: 03 May 2014

study, Takasugi et al. reported that 33 of 61 DVAs (54.1 %) had high signal intensity on 3-T MR images [7]. The etiology of the high signal intensity is uncertain, but edema, demyelination or gliosis related to venous stenosis and altered hemodynamics are possible causes [8].

DVAs are low-flow vascular malformations that are not well imaged with conventional MR sequences. Small DVAs can be easily missed on conventional MR images, and contrast-enhanced MR imaging enables better detection of DVAs [8]. Susceptibility-weighted imaging (SWI) provides unique high-resolution information on vascular lesions such as DVAs and CMs without administration of a contrast medium [9]. Recently, SWI has been used as a complementary imaging modality for identifying DVAs [7]. However, brain parenchymal signal-intensity abnormalities within the drainage territory of DVAs have not been sufficiently investigated with 3-T MR imaging. In addition, the use of high-resolution 3D fluid-attenuated inversion recovery (FLAIR) images obtained by a 3-T MR scanner may provide additional information on high-signal-intensity abnormalities within the drainage territory of DVAs because 3D FLAIR images have fewer artifacts from vessels and cerebrospinal fluid pulsation and fewer partial volume effects than 2D FLAIR images, and thus may increase the detection of subtle high-signal-intensity abnormalities [10, 11]. So far, although several reports have described the prevalence of high-signal-intensity abnormalities within the drainage territory of DVAs, there have been no reports on the size of these abnormalities. Several investigators have suggested that DVA-associated high-signal-intensity abnormalities could harbor a similar physiology to leukoaraiosis, which is common in elderly individuals [6, 8]; therefore, combined study of the size of high-signal-intensity abnormalities and patient age may provide new insight into their etiology.

In this study we used 3-T 3D FLAIR imaging to identify and evaluate the size of parenchymal high-signal-intensity abnormalities within the drainage territory of DVAs identified by 3-T SWI in a large number of patients, and assessed the association between DVA-associated high-signal-intensity abnormalities and demographic and clinical factors such as patient age, DVA location (supratentorial or infratentorial), and the presence of hypointense foci (i.e., microhemorrhages or CMs).

## Materials and methods

### Patients

This study was approved by the ethics committee of our university and the requirement for written informed consent was waived because of the retrospective study design. We retrospectively identified all MR imaging reports between January 2008 and November 2013 that contained a diagnosis of "venous angioma" or "developmental venous anomalies". Diagnosis was principally based on the presence of a cluster of venous radicals on SWI that converged into a collecting vein. Thirty-seven cases that were not studied using SWI and 3D FLAIR MR protocols were excluded. Four additional cases were excluded: three because MR image quality was not sufficient for evaluation due to motion or susceptibility artifacts and one because the patient had multiple sclerosis and a demyelinating lesion was found adjacent to the DVA. Eventually, 137 DVAs identified by SWI in 130 patients (73 men and 57 women; mean age, $55.7 \pm 18.6$ years, age range 2–88 years) were included in the study. Clinical indications are summarized in Table 1.

### MR sequences

Images were obtained using three different 3-T MR scanners: the Magnetom Verio (Siemens Medical Solutions, Erlangen, Germany) with a 32-channel phased-array head coil, the Achieva (Philips Health Care, Best, The Netherlands) with a 32-channel phased-array head coil, and the Ingenia (Philips Health Care, Best, The Netherlands) with an NVC-Base (d Stream) coil. Thirty-four patients were imaged with the Magnetom Verio, 64 patients with the Achieva, and 32 patients with the Ingenia.

The Magnetom Verio scanner performed SWI using the following parameters: TR, 25 ms; TE, 20 ms; flip angle, 16°; FOV, 21 cm; matrix size, $510 \times 512$; section

**Table 1** Clinical indications for MR examinations in all patients with DVAs ($n = 130$)

| Clinical indication | Patients |
|---|---|
| Cerebral vascular disorder | 49 |
| Brain tumor | |
| Primary brain tumor | 18 |
| Brain metastasis | 21 |
| Degenerative disease | |
| Dementia | 8 |
| Others | 1 |
| Medical checkup of the brain | 9 |
| Trauma | 5 |
| Mental disorder | 7 |
| Brain aneurysm | 4 |
| Head and neck tumor | 2 |
| Demyelinating disease | 2 |
| Hydrocephalus | 2 |
| Others | 2 |

thickness, 0.8 mm; acquisition time, 4 min 15 s. The Achieva and Ingenia scanners performed SWI using the following parameters: TR, 21–25 ms; TE, 32–37 ms; flip angle, 20°; FOV, 25 cm, matrix size, 512 × 320; section thickness, 0.8 mm; acquisition time, from 4 min 13 s to 5 min 12 s.

The 3D FLAIR sequences were obtained using 3D variable refocusing flip angles by all three MR machines. This is based on a fast spin echo (FSE; or turbo spin echo) acquisition sequence and modulates the refocusing flip angles with short echo spacing to allow longer echo train read-outs and reduce signal loss (VISTA, Philips; SPACE, Siemens). The Magnetom Verio scanner performed 3D FLAIR imaging using the following parameters: TR, 10,000 ms; TE, 625 ms; TI, 2,550 ms; turbo factor, 105; GRAPPA acceleration factor, 3; FOV, 23.5 cm; matrix size, 256 × 256; section thickness, 0.8 mm; acquisition time, 5 min. The Achieva and Ingenia scanners performed 3D FLAIR imaging using the following parameters: TR, 6,000 ms; TE, 310 ms; TI, 2,000 ms; turbo factor, 203; SENSE factor, 3; FOV, 25 cm; matrix size, 480 × 256; section thickness, 1.14 mm; acquisition time, 5 min 30 s. Axial 3D FLAIR images and axial SWI images were used in the evaluation of DVAs and associated parenchymal abnormalities.

Other MR imaging sequences performed included axial 2D FSE T2-weighted sequences (Philips; section thickness/intersection gap 5/1 mm, Siemens; section thickness/intersection gap 3/0.9 mm), single-shot echo-planar diffusion-weighted sequences, 3D FSE T1-weighted sequences, and 3D gradient-echo contrast-enhanced T1-weighted sequences. 3D gradient-echo contrast-enhanced T1-weighted images with a standard dose of contrast medium were obtained in 50 cases.

### Image analysis

MR images were reviewed by two experienced neuroradiologists who were blinded to the patients' clinical information. 3D FLAIR images were evaluated for the presence of high-signal-intensity abnormalities within the drainage territory of the DVA. SWI images were evaluated for the presence of hypointense foci (i.e., microhemorrhages or CMs) within the drainage territory of the DVA. The drainage territory was defined as the brain parenchyma directly adjacent to the visualized radicals of the DVA. Care was taken not to include signal intensities within the visible vascular structures of the DVA. The size of any high-signal-intensity abnormality on the 3D FLAIR image was quantified by measuring the maximum diameter of the lesion. The size of any high-signal-intensity abnormality on the 2D FSE T2-weighted image was also quantified by measuring the maximum diameter of the lesion when available. DVA location was classified as supratentorial (cerebrum) or infratentorial (brainstem and cerebellum). The degree of underlying white matter disease was classified as none, minimal (≤ 15 foci of abnormal hyperintensity), mild (16–35 foci), or severe (≥ 36 foci or confluent abnormal high signal intensity). Imaging findings were determined by consensus between the two neuroradiologists.

### Statistical methods

Patient age was compared across DVAs with and without high-signal-intensity abnormalities within the drainage territory using a *t*-test. The presence of hypointense foci on SWI, DVA location, and the extent of underlying white matter disease were compared across DVAs with and without high-signal-intensity abnormalities within the drainage territory using Fisher's exact tests. The correlation between the size of the high-signal-intensity abnormality and patient age was evaluated using linear regression analysis. All analyses were performed for all DVAs ($n = 137$) and for the subgroup of DVAs that had no or minimal underlying white matter disease ($n = 71$). Values of $p < 0.05$ were considered statistically significant. Statistical analysis was performed using commercially available software (SPSS 21.0, Chicago, IL, USA).

## Results

Of the 137 DVAs identified, 42 (30.7 %) had high-signal-intensity abnormalities within the drainage territory. An adjusted prevalence rate of 18/71 (25.4 %) was obtained when only patients with no or minimal underlying white matter disease were considered. Twenty of the 137 DVAs (14.6 %) had hypointense foci within the drainage territory on SWI.

Tables 2 and 3 outline the association between high-signal-intensity abnormalities and other factors in the full sample of DVAs ($n = 137$; Table 2) and the subgroup of DVAs with no or minimal underlying white matter disease ($n = 71$; Table 3). DVA location was associated with the presence of high-signal-intensity abnormalities in both the full sample and the subgroup (both $p < 0.05$), indicating that high-signal-intensity abnormalities were more frequently encountered in supratentorial regions than in infratentorial regions. In the supratentorial location, high-signal-intensity abnormalities were exclusively found in white matter. In the infratentorial location, only a single case showed a high-signal-intensity abnormality, and this was in the middle cerebellar peduncle. The presence of hypointense foci, patient age, and the degree of underlying white matter disease had no association with the presence

**Table 2** Association between high-signal-intensity abnormalities within the DVA drainage territory and other factors in the full sample of DVAs

| Full sample ($n = 137$) | | | | |
|---|---|---|---|---|
| Factor | High-signal-intensity abnormality | | Total | $p$ value |
| | Yes | No | | |
| Hypointense foci | | | | 0.065 |
| No | 32 | 85 | 117 | |
| Yes | 10 | 10 | 20 | |
| Location | | | | <0.05[b] |
| Supratentorial | 41 | 43 | 84 | |
| Infratentorial | 1 | 52 | 53 | |
| White matter disease | | | | 0.18 |
| None | 9 | 29 | 38 | |
| Minimum | 9 | 24 | 33 | |
| Moderate | 3 | 13 | 16 | |
| Severe | 21 | 29 | 50 | |
| Age[a] | (59.3 ± 17.4)[c] | (53.3 ± 19.5)[c] | | 0.094 |

[a] Patient age was compared across DVAs with and without high-signal-intensity abnormalities within the drainage territory using a $t$-test. The presence of hypointense foci, DVA location, and the degree of white matter disease were compared across DVAs with and without high-signal-intensity abnormalities within the drainage territory using Fisher's exact tests

[b] DVA location was associated with the presence of high-signal-intensity abnormalities

[c] Values in parentheses are mean and standard deviations

of high-signal-intensity abnormalities within the drainage territory of DVAs.

The maximum diameter of the high-signal-intensity abnormalities on 3D FLAIR images was 13.5 ± 7.9 mm for the full sample and 8.3 ± 6.7 mm for the subgroup. There was a significant correlation between the size of the high-signal-intensity abnormality on 3D FLAIR images and patient age in the full sample ($R^2 = 0.3602$, $p < 0.01$; Fig. 1a) and in the subgroup ($R^2 = 0.423, p < 0.01$; Fig. 1b), whereby the high-signal-intensity abnormality was larger in older patients. All patients with a high-signal-intensity abnormality ≤ 6 mm in maximum diameter were under 40 years of age. MR images of representative cases are shown in Figs. 2 and 3. 2D FSE T2-weighted images were available in 39 of the 42 cases with high-signal-intensity abnormalities within the drainage territory of the DVA. High-signal-intensity abnormalities ≤ 2.3 mm in maximum diameter on 3D FLAIR ($n = 4$) were not detected on 2D FSE T2-weighted images, but high signal lesions ≥ 4 mm maximum diameter on 3D FLAIR ($n = 35$) were all detected on 2D FSE T2-weighted images. The maximum diameter of the high-signal-intensity abnormalities on the 2D FSE T2-weighted images in these 35 cases was 13.5 ± 7.5 mm.

**Table 3** Associations between high-signal-intensity abnormalities within the DVA drainage territory and other factors in the subgroup of DVAs with no or minimal underlying white matter disease

| Subgroup ($n = 71$) | | | | |
|---|---|---|---|---|
| Factor | High-signal-intensity abnormality | | Total | $p$ value |
| | Yes | No | | |
| Hypointense foci | | | | 0.26 |
| No | 14 | 47 | 61 | |
| Yes | 4 | 6 | 10 | |
| Location | | | | <0.05[b] |
| Supratentorial | 17 | 30 | 47 | |
| Infratentorial | 1 | 23 | 24 | |
| Age[a] | (47.4 ± 19.1)[c] | (46.1 ± 19.9)[c] | | 0.79 |

The subgroup includes patients with no or minimal white matter disease

[a] Patient age was compared across DVAs with and without high-signal-intensity abnormalities within the drainage territory using a $t$-test. The presence of hypointense foci and DVA location were compared across DVAs with and without high-signal-intensity abnormalities within the drainage territory using Fisher's exact tests

[b] DVA location was associated with presence of high-signal-intensity abnormalities

[c] Values in parentheses are mean and standard deviations

## Discussion

SWI combines the detailed spatial resolution of 3D gradient-echo imaging with the ability to detect blood with a reduced oxygenation level. This unique description of anatomical and physiological features makes it possible to investigate slow-flow vascular malformations such as DVAs and CMs as well as small hemorrhages [9]. Other non-contrast MR sequences including spin-echo sequences, time-of-flight MR angiography or venography, and 2D T2*-weighted gradient-echo techniques are suboptimal for identifying malformed vessels that exhibit slow multidirectional flow [12]. Thus, SWI appears optimal for identifying DVAs and related CMs or small hemorrhages.

This study focused on parenchymal abnormalities within the drainage territory of DVAs that were identified by SWI. Four studies, including ours, have reported the prevalence of high-signal-intensity abnormalities within the drainage territories of DVAs [6–8]. The prevalence reported in previous studies was variable, ranging from 7.8 to 54.1 %. In our study, high-signal-intensity abnormalities were present in 30.7 % of DVAs and 24.3 % of a subgroup of DVAs that had no or minimal underlying white matter disease. Compared to the three previous studies, our study had the second-largest number of DVAs. The remaining two studies had a relatively small number of DVAs ($n = 60$ and 61 for references [6] and [7], respectively).

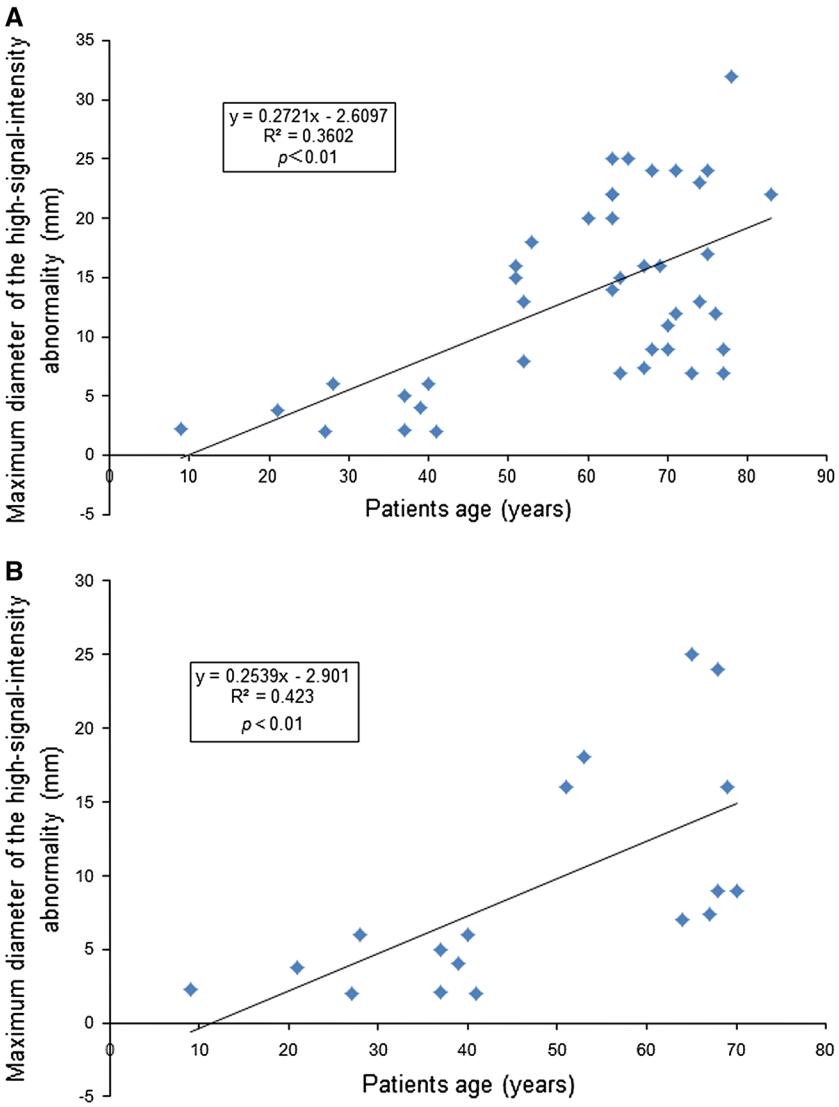


**Fig. 1** The linear relation between patient age and the size of high-signal-intensity abnormalities within the drainage territory of DVAs in the full sample (**a**) and the subgroup of DVAs with no or minimal underlying white matter disease (**b**)

Moreover, in these two studies, no mention was made of exclusion criteria related to potential signal intensity changes associated with adjacent non-related pathology [6], and no attempt was made to control for more widespread white matter signal intensity alterations that are common in elderly patients [6, 7]. The MR imaging methods used to identify DVAs were variable, and included contrast-enhanced MR imaging in two studies [6, 8] and SWI in one study [7]. Therefore, variation in the reported prevalence may be due to varying inclusion and exclusion criteria, the number of patients studied, and the MR imaging methods. Nonetheless, the high prevalence of high-signal-intensity abnormalities within the drainage territory of DVAs should be noted, as everyday clinical experience indicates that increasing use of SWI will bring more opportunities for identifying DVAs.

In the present study, high-signal-intensity abnormalities within the drainage territory of DVAs were exclusively evaluated using 3D FLAIR images. Previous investigations have used 2D FLAIR images or 2D FSE T2-weighted images to evaluate the presence of high-signal-intensity abnormalities [6–8], and there are no previous reports on the use of 3D FLAIR images for the detection of high-signal-intensity abnormalities within the drainage territory of DVAs. Kakeda et al. reported that the conspicuity and detection of most brain lesions on 3D FLAIR images were equal or superior to that on 2D FLAIR images, and the mean contrast ratio was higher on 3-T 3D FLAIR images than on 3-T 2D FLAIR images [13]. In addition, the use of thin-slice 3D FLAIR images leads to more precise detection and evaluation of small high-signal-intensity abnormalities, as our results showed that high-signal-intensity abnormalities $\leq$ 2.3 mm in maximum diameter were detected only on 3D FLAIR images. Consequently, the use of high-resolution 3D FLAIR imaging in the current study allowed us to identify small

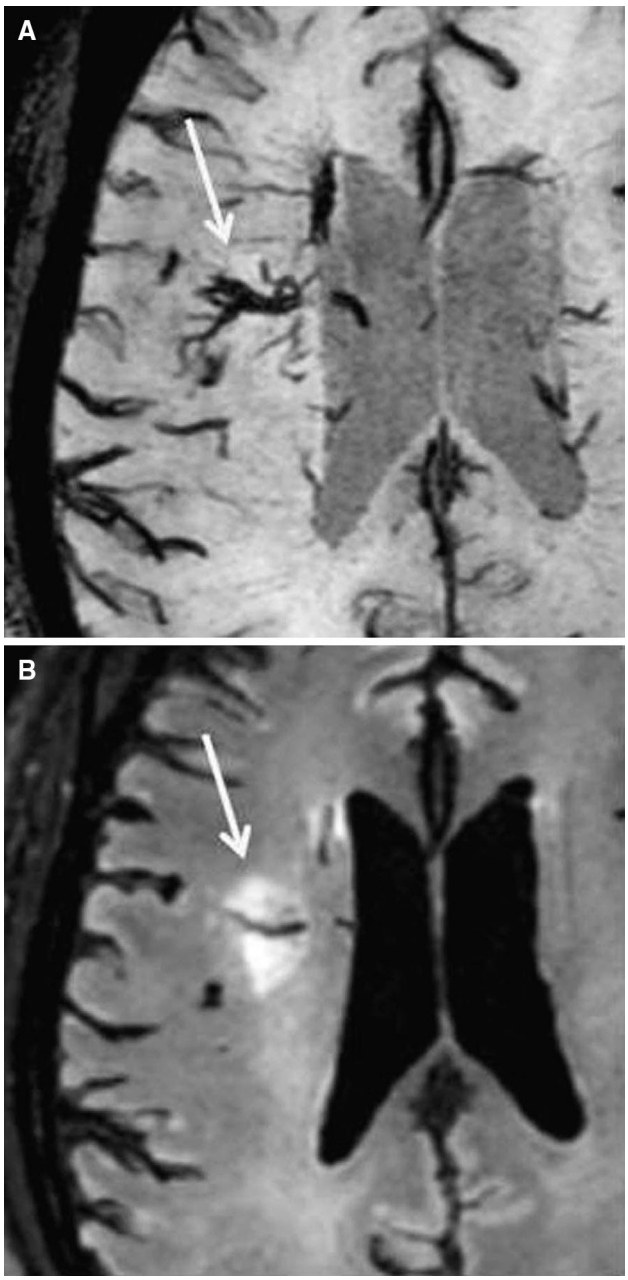


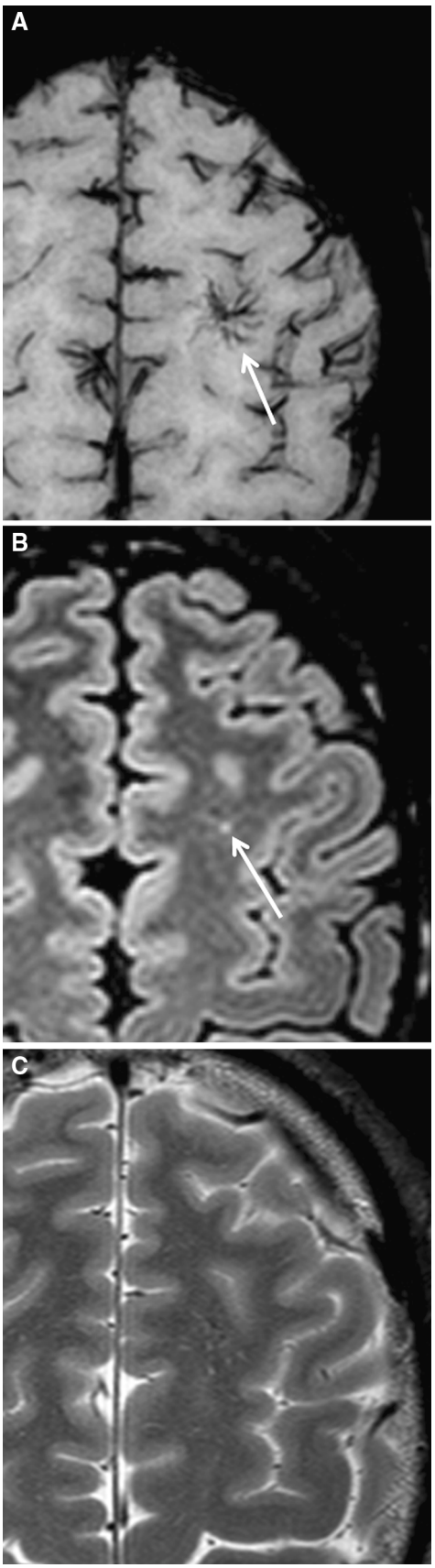


**Fig. 2** SWI (**a**) and 3D FLAIR (**b**) images from a 60-year-old male with a DVA in the right frontal lobe (*arrow* on **a**). The 3D FLAIR image shows a large, classic high-signal-intensity abnormality within the drainage territory of the DVA, extending into the white matter (*arrow* on **b**). The maximum diameter of the high-signal-intensity abnormality was 20 mm

DVA-associated high-signal-intensity abnormalities and to evaluate the size of these lesions.

The etiology of high-signal-intensity lesions remains uncertain. The pathology of the lesions also remains unknown, but some possibilities include gliosis, demyelination or edema due to chronic mild venous hypertension caused by anomalous venous drainage [14]. Santucci et al.

◀**Fig. 3** SWI (**a**), 3D FLAIR (**b**) and 2D FSE T2-weighted (**c**) images from a 27-year-old female with a DVA in the left frontal lobe (*arrow* on **a**). The 3D FLAIR image shows a small high-signal-intensity abnormality within the drainage territory of the DVA (*arrow* on **b**). The maximum diameter of the high-signal-intensity abnormality was 2 mm. The 2D FSE T2-weighted image fails to show a high-signal-intensity abnormality

reported that DVAs with high-signal-intensity abnormalities were more common in older patients than in younger patients [8]. However, we found no significant difference in the age of patients with and without DVA-associated high-signal-intensity abnormalities. This may be due to the use of high-resolution 3D FLAIR images for the evaluation of high-signal-intensity abnormalities in the current study. The size of high-signal-intensity abnormalities was larger in older patients, and lesions $\leq$ 6 mm in maximum diameter were exclusively found in patients less than 40 years of age. In addition, we found that high-signal-intensity abnormalities with maximum diameter $\leq$ 2.3 mm on 3D FLAIR images were not detected on 2D FSE T2-weighted images. Therefore, our results suggest that high-resolution 3D FLAIR imaging identifies small high-signal-intensity abnormalities in younger patients that may not be detected with 2D imaging sequences.

It remains unknown whether individual DVAs grow slowly over a long period or whether they suddenly appear and evolve rapidly as an acute infarct. We did not follow individual DVA cases for sufficiently long periods to address this question, as our cases were followed for 3 years at most. Nevertheless, our results suggest that high-signal-intensity abnormalities may increase in size with aging. The term leukoaraiosis (from the Greek *leuko*, meaning white, and *araiosis*, meaning rarefaction) was introduced by Hachinski to designate bilateral and symmetrical areas in the periventricular and centrum semiovale white matter that showed hypodensity on CT and hyperintensity on T2-weighted images [15, 16]. Leukoaraiosis is an age-related neurodegenerative condition that appears as an area of hyperintense signal in the white matter on MR images as a result of white matter ischemia. It is characterized histologically by demyelination, loss of glial cells, and vacuolization [17]. Moody et al. reported that there might be a mechanistic link between leukoaraiosis and collagenous thickening of venous walls, rather than an incidental association [18]. The increased resistance to venous blood flow that results from venous stenosis might induce chronic ischemia and/or edema in the deep white matter, leading to leukoaraiosis [19]. High-signal-intensity abnormalities within the drainage territory of DVAs might have a similar pathophysiology.

In the current study, no DVAs in the cerebellar hemisphere had high-signal-intensity abnormalities within the drainage territory. We cannot clearly explain this observation. Takasugi et al. presented a case with DVA-related high-signal-intensity abnormalities in cerebellar white matter [7], although the total number of DVA cases with cerebellar high-signal-intensity abnormalities was not given in their results. On the other hand, San Millán Ruíz et al. did not observe any cerebellar white matter abnormalities [6], and Santucci et al. did not observe any cerebellar high-signal-intensity abnormalities after excluding cases with significant underlying white matter disease [8]. These results are consistent with ours, and may support the hypothesis that the pathophysiology of DVA-associated high-signal-intensity abnormalities is similar to that of leukoaraiosis, although further investigations with more cases are necessary to confirm this**.** If this hypothesis is correct, altered hemodynamics and increased susceptibility to ischemia due to aging may be one reason for the association between the size of any high-signal-intensity abnormality and patient age. Consequently, it is possible to speculate that a small high-signal-intensity abnormality, such as one with a maximum diameter $\leq$ 6 mm, might be an early indication of a large and classic high-signal-intensity abnormality.

We used 3-T SWI to detect hypointense foci that suggested microhemorrhage or CM. SWI is sensitive to the presence of even small amounts of hemorrhage. In addition, 3-T MR imaging is sensitive to the susceptibility effect, increasing the detection of hypointense foci. However, the prevalence of hypointense foci was 14.6 % in the current study, almost the same as the prevalence (up to 18 %) reported in previous studies that used 2D gradient-echo imaging at 1.5 T [8, 20], and much lower than the prevalence reported by Takasugi et al. (62.3 %) using SWI at 3 T [7]. The reason for this discrepancy is unknown. Takasugi et al. also reported that hypointense foci showed a significant association with high-signal-intensity abnormalities within the drainage territory of DVAs on 2D FSE T2-weighted images. However, our results showed no significant association between hypointense foci and high-signal-intensity abnormalities. Further studies with a large number of cases using SWI and high-resolution 3D FLAIR imaging are necessary to clarify the association between hypointense foci and high-signal-intensity abnormalities within the drainage territory of DVAs.

This study has several limitations. First, although our study population was relatively large in comparison to previous studies [6–8], more cases may be necessary to confirm the finding that the size of high-signal-intensity abnormalities is correlated with patient age. Second, we did not longitudinally study changes in the size of high-signal-intensity abnormalities because we did not have data on 3D FLAIR examinations over a sufficiently long period. This is due to the fact that 3-T 3D FLAIR imaging started only

5 years ago in our institution. In the future it will be possible to observe changes in the size of DVA-associated high-signal-intensity abnormalities over longer time periods.

In conclusion, 3D FLAIR imaging at 3 T permits detection of small high-signal-intensity abnormalities within the drainage territory of DVAs, and our results suggest that the size of high-signal-intensity abnormalities increases with patient age. However, further investigations with more cases are necessary to clarify the correlation between patient age and the size of DVA-associated high-signal-intensity abnormalities.

**Conflict of interest** Maki Umino: the authors declare that they have no conflict of interest.

## References


1. Wilms G, Bleus E, Demaerel P, Marchal G, Plets C, Goffin J, et al. Simultaneous occurrence of developmental venous anomalies and cavernous angiomas. AJNR Am J Neuroradiol. 1994;15:1247–54.
2. Huber G, Henkes H, Hermes M, Felber S, Terstegge K, Piepgras U. Regional association of developmental venous anomalies with angiographically occult vascular malformations. Eur Radiol. 1996;6:30–7.
3. Abe T, Singer RJ, Marks MP, Norbash AM, Crowley RS, Steinberg GK. Coexistence of occult vascular malformations and developmental venous anomalies in the central nervous system: MR evaluation. AJNR Am J Neuroradiol. 1998;19:51–7.
4. Lasjaunias P, Burrows P, Planet C. Developmental venous anomalies (DVA): the so-called venous angioma. Neurosurg Rev. 1986;9:233–42.
5. Okudera T, Huang YP, Fukusumi A, Nakamura Y, Hatazawa J, Uemura K. Micro-angiographical studies of the medullary venous system of the cerebral hemisphere. Neuropathology. 1999;19:93–111.
6. San Millán Ruíz D, Delavelle J, Yilmaz H, Gailloud P, Piovan E, Bertramello A. Parenchymal abnormalities associated with developmental venous anomalies. Neuroradiology. 2007;49:987–95.
7. Takasugi M, Fujii S, Shinohara Y, Kaminou T, Watanabe T, Ogawa T. Parenchymal hypointense foci associated with developmental venous anomalies: evaluation by phase-sensitive MR imaging at 3T. AJNR Am J Neuroradiol. 2013;34:1940–4.
8. Santucci GM, Leach JL, Ying J, Leach SD, Tomsick TA. Brain parenchymal signal abnormalities associated with developmental venous anomalies: detailed MR imaging assessment. AJNR Am J Neuroradiol. 2008;29:1317–23.
9. Reichenbach JR, Jonetz-Mentzel L, Fitzek C, Haacke EM, Kido DK, Lee BC, et al. High-resolution blood oxygen-level dependent MR venography (HRBV): a new technique. Neuroradiology. 2001;43:364–9.
10. Kitajima M, Hirai T, Shigematsu Y, Uetani H, Iwashita K, Morita K, et al. Comparison of 3D FLAIR, 2D FLAIR, and 2D T2-weighted MR imaging of brain stem anatomy. AJNR Am J Neuroradiol. 2012;33:922–7.
11. Kallmes DF, Hui FK, Mugler JP 3rd. Suppression of cerebrospinal fluid and blood flow artifacts in FLAIR MR imaging with a single-slab three-dimensional pulse sequence: initial experience. Radiology. 2001;221:251–5.
12. Thomas B, Somasundaram S, Thamburaj K, Kesavadas C, Gupta AK, Bodhey NK, et al. Clinical applications of susceptibility weighted MR imaging of the brain—a pictorial review. Neuroradiology. 2008;50:105–16.
13. Kakeda S, Korogi Y, Hiai Y, Ohnari N, Sato T, Hirai T. Pitfalls of 3D FLAIR brain imaging: a prospective comparison with 2D FLAIR. Acad Radiol. 2012;19:1225–32.
14. Noran HH. Intracranial vascular tumors and malformations. Arch Pathol Lab Med. 1945;39:393–416.
15. Hachinski VC, Potter P, Merskey H. Leuko-araiosis: an ancient term for a new problem. Can J Neurol Sci. 1986;13:533–4.
16. Hachinski VC, Potter P, Merskey H. Leuko-araiosis. Arch Neurol. 1987;44:21–3.
17. Munoz DG, Hastak SM, Harper B, Lee D, Hachinski VC. Pathologic correlates of increased signals of the centrum ovale on magnetic resonance imaging. Arch Neurol. 1993;50:492–7.
18. Moody DM, Brown WR, Challa VR, Anderson RL. Periventricular venous collagenosis: association with leukoaraiosis. Radiology. 1995;194:469–76.
19. Brown WR, Moody DM, Challa VR, Thore CR, Anstrom JA. Venous collagenosis and arteriolar tortuosity in leukoaraiosis. J Neurol Sci. 2002;15:159–63.
20. Töpper R, Jürgens E, Reul J, Thron A. Clinical significance of intracranial developmental venous anomalies. J Neurol Neurosurg Psychiatry. 1999;67:234–8.